7828 *Macromolecules* **2010**, *43*, 7828–7838
DOI: 10.1021/ma101091k

Macromolecules
ARTICLE

Poly(styrenesulfonate)−Poly(diallyldimethylammonium) Mixtures: Toward the Understanding of Polyelectrolyte Complexes and Multilayers via Atomistic Simulations

Baofu Qiao,* Juan J. Cerdà, and Christian Holm*

Institute for Computational Physics. Universität Stuttgart. 70569 Stuttgart, Germany

Received May 18, 2010; Revised Manuscript Received August 11, 2010

ABSTRACT: Explicit solvent all-atom molecular dynamics simulations of mixtures of poly(styrenesulfonate)-(PSS) and poly(diallyldimethylammonium) (PDADMA) polyelectrolytes at various salt (NaCl) concentrations are performed. We characterize the formed polyelectrolyte complexes (PECs) and relate the observed physical properties of PSS−PDADMA PECs to the properties found in polyelectrolyte multilayers (PEMs) made of the same compositions. Our results reveal a change in the way charges are compensated upon the addition of salt, namely from an intrinsic mechanism (polyanions pair with polycations) toward an extrinsic one (polyions pair with salt ions). The probability of the intrinsic compensating mechanism decreases from about 90% to about 60% when the salt concentration increases from 0.168 to 1 mol/L. The interaction energies of the ion-pairing follow the order of Na−Cl > PSS−Na > PDADMA−Cl≅PSS−PDADMA. Furthermore, we investigate thoroughly the water distribution and study the hydration mechanisms in our system. Water is found to be homogeneously distributed inside our investigated systems, while we find a negligible difference between the hydration ability of (PDADMA + Cl^-) and (PSS + Na^+). This lack of asymmetric behavior demonstrates that the observed swelling−shrinking switch during the buildup of PEMs cannot be related to the hydration behavior, and we suggest that the presence of a substrate has to play a critical role. A further analysis of the water structure shows that the dielectric constant inside such mixtures is roughly 1 order of magnitude lower than in bulk water, and our determined values compare favorably with experimental measurements. Finally the diffusion of water molecules inside the PE mixtures is found to be 2 orders of magnitude slower than that in pure water.

I. Introduction

Polyelectrolyte multilayers (PEMs) are composed of alternating layers of oppositely charged polyelectrolytes (PEs) (synthetic PEs or biomolecules), which are generally built up based on the layer-by-layer technique.[1,2] PEMs have stimulated great interests from both academic researchers and industries due to their potential applications, such as membrane, encapsulation, and matrix materials for enzymes and proteins in sensor applications. The current knowledge about the applications, structure and synthesis of PEMs has been gathered together in several recent reviews.[3−8]

Despite the large amount of experimental works, theoretical and computational studies are relatively scarce (for a review, see refs 9−11). Simulations performed so far to study PEMs are all based on coarse-grained (CG) models due to the current inability to perform all-atom (AA) simulations of such large and slowly relaxing systems. The CG models have the advantage of bigger system sizes and faster relaxation times but they do not allow for a close comparison to experiments due to several simplifications done in such models. For instance, the implicit model of the solvent and the oversimplified electrostatic landscape. In particular, it was reported very recently that the implicit solvent models may not be able to describe correctly the polyelectrolyte adsorption under poor solvent condition,[12] which can pose a serious problem in the numerical description of PEMs because most of experimental PEMs are prepared in such regime. The present work aims to go beyond traditional coarse grained simulations and we address the study of the behavior of PE mixtures as a first step toward the study of PEMs using an explicit atomistic description of the PEs, as well as of the water molecules. In addition, we expect atomistic studies to be able to provide useful information to refine and tune the potentials used in CG models (see ref 10), which would allow CG models to mimic better realistic systems under experimental conditions.

The study of the PE mixtures can be regarded as a first step toward the physical understanding of the formation and the structures of PEMs. PEMs and PE complexes (PECs) composed of poly(styrenesulfonate) (PSS) and poly(diallyldimethylammonium) (PDADMA) have been experimentally characterized using FTIR,[13] as well as ^1H[14] and ^{13}C[15] solid-state NMR. On the basis of such works, it has been concluded that the microscopic structure of PSS/PDADMA PEMs far from the substrate is very similar to that observed in PSS/PDADMA PECs. Support in favor of the close relation between PECs and PEMs composed of PSS and PDADMA has been provided by experiments[16−19] and theoretical works.[20] Nonetheless, some differences in the secondary structures of peptides has been found in poly(L-lysine)/poly(L-glutamic acid) (PLL/PLGA) systems when comparing their respective conformations inside PEMs and PECs,[21,22] which is probably related to the inter- and intramolecular hydrogen-bonding in polypeptide systems.

Several works using atomistic simulations of PECs have been intended to get insight about PEMs. Haynie et al.[23] have studied PECs composed of PLL/PLGA polypeptides, in which the peptides of 6-mer (i.e., six amino acid length) were investigated in the solvent of TIP3P waters. The hydrophobic interaction,

*Corresponding authors . E-mail: (Q.B.) qiaobf@gmail.com; (C.H.) holm@icp.uni-stuttgart.de.

 Published on Web 08/19/2010

in addition to electrostatic interaction, was found to play an important role in stabilizing the secondary structure of the β-sheet. In a subsequent work,[24] the relation between the simulational interactions of PECs and the experimental surface roughness in PEMs was also analyzed, in which the 32-mer peptides were used under both conditions. Note that an implicit solvent has been employed in ref 24. Very recently, Hoda and Larson[25] investigated the poly(styrenesulfonate)/poly(allylamine hydrochloride) (PSS/PAA) and poly(acrylic acid)/poly(allylamine hydrochloride) (PAA/PAH) PECs to the aim of understanding the growth mechanism of the corresponding PEMs (linear growth for the former and exponential growth for the later), in which PEs with a chain length of 20 monomers were discussed extensively.

In addition to the pure AA and CG models currently used in the study of PEMs, some hybrid models might also provide a useful insight. In that direction some works have been already done using explicit/implicit hybrid solvent method[26] and multiscale AA/CG hybrid method (see ref 27 and references therein). In the case of the explicit/implicit hybrid solvent methods, a work based on the PEC systems has found that by reparameterizing the force field parameters of PEs, properties like RDF and R_g obtained in the explicit solvent method could be reproduced with the implicit solvent model.[25] Reddy et al.[12] have suggested that an explicit solvent model is required for PEs adsorption on the charged or neutral substrate in poor solvent conditions. Therefore, the most reasonable use one could do of those explicit/implicit hybrid solvent models would be using the explicit method close to the substrate and the implicit model in the water buffer region. Similarly, we envision the use of AA/CG hybrid models in the study of PEMs, in which the AA model is applied to the region close to the substrate and the CG model in the water buffer region. Such types of simulations will be much closer to experiments than current simulations yet will stay within current computer capabilities.

In the present work, we want to gain a microscopic understanding of the structural properties of PEMs. Therefore, we simulate a mixture of PEs containing water and salt in concentrations close to those one can find in real PEMs. In order to get a description as accurate as possible, we opted to perform explicit solvent AA molecular dynamics simulations. The PE mixtures are expected to be closely related to the structure in the central region of PEMs, i.e., far from the substrate and the PEM interface with the bulk water solution. It is noteworthy that the previous atomistic-level simulation works[23−25] are all studying PEC systems under very dilute PE concentrations, which can behave very differently from the bulky PE mixtures investigated here. We are specifically focusing on those properties which cannot be properly investigated using the current oversimplified CG models. In particular, the properties under study include the formation of electrostatic pairs (ion-pairing), the hydration abilities of polycations and polyanions, as well as the dynamics of water molecules (diffusion constant and dielectric constant). The influence of salt ions on these properties has been also thoroughly studied.

Among the several PE combinations that have been experimentally characterized, the PSS/PDADMA combination using NaCl as salt is one of the more extensively studied systems. And as previously discussed, the similarity between the properties of PEM and PEC composed of PSS and PDADMA have been well verified. For that reason, we have decided to focus our work on PSS/PDADMA/water/NaCl mixtures.

The paper is organized as follows: In section II, the description of the systems under study and the simulation details are given. In section III, results and discussions will be provided. Finally, conclusions are presented in section IV.

II. Simulation Methodology

A. Systems under Study. One of our main reasons to study PSS/PDADMA mixtures is to gain insight about PEMs of the same composition. It is known that such PEMs contain water molecules and salt in addition to PSS and PDADMA. It would be desirable to perform a systematic study of the influence of water and salt concentration on the PSS/PDADMA PECs properties by varying both concentrations independently. However, AA molecular dynamic simulations are computationally very demanding rendering such a systematic study impossible. Recently Schlenoff and co-workers[28] have experimentally performed quantitatively studies of salt and water concentrations in PSS/PDADMA PEMs using doping equilibrium method. Therefore, in the present work, we will use concentrations of water and NaCl inspired by their work.

Table 1. Compositions of the Systems under Study

	number of components[a]				concentration[b]	
mixture	PSS	PDADMA	H_2O	NaCl	c_{PE}	c_{NaCl}
i	35	35	2940	25	2.82	0.168
ii	35	35	3738	82	2.56	0.500
iii	35	35	4536	180	2.33	1.000

[a] Degree of polymerization is 12 for both PSS and PDADMA. [b] Unit: mol/L. Standard deviation are less than 0.2%.

In PEM experiments, the degree of polymerization (DP) of PEs are generally in the range 100−1000, which is far beyond our current computer capabilities. Because of the electrostatic interactions, the diffusion of the PEs are so low that it is difficult for atomistic simulations event to equilibrate such systems. In general, the higher the DP is, the longer a simulation must be run to reach the equilibrium state. In the present work, we use a DP = 12 for both PSS and PDADMA as a compromise between the computer resources and getting as close as possible to real experiments. Considering that the persistence length of PSS is about 1.4 nm[25] and the contour length of PSS with DP = 12 is about 3.5 nm, the considered PSSs behave rodlike.

In order to assess the effects of the chain length on the physics of the PE mixtures, we have carried out preliminary investigations using several DPs with the remaining parameters kept equal to those of system (i) (see Table 1). The observed dielectric constant of waters are $\epsilon = 16.1 \pm 0.5$, 11.6 ± 1.3, 10.3 ± 0.9, 10.9 ± 0.6, 11.7 ± 1.4, for the different values of DP= {1, 3, 5, 10, 12}. Our test shows that differences between the dielectric constants are very small when DP $\geq$ 3. Furthermore, very recently Spruijt and co-workers[29] have experimentally investigated the dependence of the structures of strongly charged poly(acrylic acid)(PAA)/poly(*N*,*N*-dimethylaminoethyl methacrylate) (PDMAEMA) PECs on four different DPs (20, 50, 150, and 510) of both polycation and polyanion. The water contents inside the PECs were found to be independent of DP, and to increase with increasing salt concentration, and similar findings are expected in other strongly charged PECs.[29] Hence the calculated properties in PSS/PDADMA, both of which are strong PEs, in the present work may not be expected to depend strongly on the DP chosen.

We also remark here that although longer PE chains have been simulated in previous atomistic works, some simplifications were applied: (a) in ref 24, peptides of DP = 32 are used in combination with implicit solvent model; (b) in ref 25, the PEs were modeled at united-atom level. The detailed discussions were based on chains with DP = 20 at very dilute PE concentrations ($\sim 10^{-4}$ mol/L in monomer unit), and they studied the structures of PSS/PAH and PAA/PAH PECs under different DPs at the absence of both PE counterions and salt ions; (c) a shorter PSS chain of DP = 8 has been applied to study the adsorption on graphene surfaces at the united-atom level.[30]

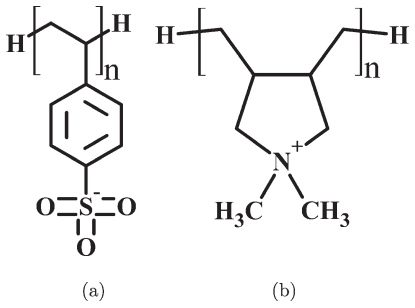

Figure 1. Schematic representation of PSS (a) and PDADMA (b). In the simulations, the degree of polymerization is $n = 12$.

The chemical structures of PSS (polyanion) and PDADMA (polycation) are depicted in Figure 1. It should be noticed that in the case of PDADMA two different monomer conformations are possible due to the relative position of the allyl groups (*trans* or *cis*). In order to get closer to the experiments, we set the ratio *trans:cis* to be 6:1 (see refs 31 and 32), that is, all the monomers from 30 (out of 35) PDADMA chains are in the *trans* conformation, and all the others are in the *cis* conformation.

The amount of salt (NaCl in the present work) and water is set based on the experimental determinations of Schlenoff et al.[28] mentioned above. The compositions of our PE mixtures are summarized in Table 1. It should be mentioned that, in ref 28, the concentrations of water and salt were obtained for PEMs in equilibrium with a water buffer: the salt concentration refers to that in the water buffer region, while the water concentration is the one inside PEMs, and therefore our concentrations are only a rough approximation to those one could expect to have inside PEMs. The main approach we do is to assume that the salt concentration inside and outside PEMs are roughly similar and the osmotic equilibrium do not substantially bias them. To our best knowledge, no experimental determination of both the contents of water and salt inside PEMs is available. It would be highly desirable to have experimental works performed in such direction in order to have a more accurate ratio of salt to water in PEMs simulations.

B. Simulation Details. Classical molecular dynamics (MD) simulations are performed using the package GROMACS 4.0.5.[33] We used the leapfrog algorithm and a time step of 2 fs. All covalent bonds involving hydrogens are constrained using the LINCS algorithm.[34] Because of the ability to reproduce the hydration behavior and the dielectric constant of waters,[35] the SPC/E water model[36] is chosen, the geometry of which are fixed with the SETTLE algorithm.[37] The other force field parameters are based on the OPLS-AA force field.[38] See the Supporting Information for the OPLS-AA potential energy. Because of the lack of force field parameters (i.e., the partial charge) of diallyldimethylammonium and sulfonate groups in the OPLS-AA, some modifications have been performed based on the original OPLS-AA force field:

- PSS: the partial charges of sulfur and oxygen from the sulfonate groups are based on that of a neutral charged and related group, i.e., sulfonamide ($-S(=O)_2OR$). In order to guarantee that the total charge was -1 *e*, the partial charge of the benzene carbon chemically bonded to the sulfur atom has been modified from 0 to -0.44 *e*. To test the modified force field for PSS, two calculations have been performed: (a) Radial distribution functions (RDFs) from a system composed of a 10-mer PSS are obtained under the same concentrations of K^+ and water as those in ref 39, where the force field for PSS was developed at the united-atom level. Both of the calculated RDFs (between sulfonate sulfur and K^+, and between sulfonate oxygen and water oxygen) agree well with the reported RDFs in ref 39. See Figure S1 in the Supporting Information. (b) Radius of gyration R_g of a 10-mer PSS has been calculated under the same concentrations of Na^+ and water as those applied in ref 25. Our measurement yielded a value of $R_g = 0.72 \pm 0.04$, which agrees well with the united-atom level simulational value of $R_g = 0.74$,[25] and a value of 0.66 nm predicted based on an experiment(see ref 84 in ref 25). Such agreements support that the present force field for PSS is able to substantially catch the feature of PSS. Note that a very precise force field need the comparison with experimental data, which are lack for PSS so far.
- PDADMA. The partial charges of PDADMA are taken from ref 40: nitrogen -0.32 *e*, carbon of the methyl groups 0.15 *e*, carbons in the ring bonded to the nitrogen 0.21 *e*, and hydrogens 0.06 *e*.

In order to obtain a properly equilibrated system, the following protocol is followed in all our simulations: The initial systems are built using the package Packmol.[41,42] An initial cubic box of 40 nm is set and the polyelectrolyte molecules are located inside an inner cubic region of side 30 nm centered within the box. Water molecules and ions are placed in the remaining empty space surrounding the inner region.

In the next stage we perform an annealing of the polyelectrolyte molecules keeping the waters and salt ions fixed at their original positions. The temperature is lowered in successive steps of 1 ns to 500 K, 400 K, 350 K, and finally 298 K. Once the annealing has been finished, a pressure of 500 bar is applied for a duration of 6 ns to force the waters and salt ions to protude inside the polyelectrolyte mixture and get a conformation closer to the one we expect inside PEMs. In the subsequent stage, four thermal cycles of 14 ns each are performed in order to ensure that initial correlations among molecules disappear. In each thermal cycle the temperatures are changed at regular intervals according to the following ascendent-descendent temperature profile: {298 K, 350 K, 400 K, 350 K, 298 K}. Followed by every thermal cycle is a simulation performed at 298 K, in which the potential energy is recorded. The monitoring of the potential energy of the system shows that after one or two of those thermal cycles the system is already at equilibrium. During those thermal cycles, in order to speed up the process of accommodation of the system, a cutoff method is used to deal with the electrostatic interactions. After completion of the four cycles, the long-range electrostatic interaction is imposed using the particle mesh Ewald (PME) method,[43,44] and the system is then run by another period of 10 ns to equilibrate.

The production stage last for 100 ns, where the isobaric−isothermal ensemble is used and the temperature is scaled via a Nose−Hoover thermostat (characteristic time $\tau = 0.5$ ps) which is used in combination with a Parrinello−Rahman barostat algorithm (characteristic time $\tau = 4$ ps, reference pressure 1 bar, compressibility 4.5×10^{-5} bar^{-1}). The neighbor searching is done up to 1.2 nm, and updates are performed each 10 time steps. LJ interactions and forces are also cutoff at 1.2 nm. The long-range interactions are handled via PME method with a direct space cutoff of 1.2 nm and Fourier grid spacing 0.12 nm. Long-range dispersion corrections for the energy and pressure are applied. Each 1 ps a conformation is recorded to perform the subsequent analysis.

Table 2. Calcualted Results of Several Observables

mixture	potential, kJ/mol	volume, nm^3	slow dynamics of H_2O: ϵ^b	slow dynamics of H_2O: diffusion coefficient[c]
i[a]	-208400 ± 600	247.7 ± 0.4	11.7 ± 1.4	3.61 ± 0.01
	-208400 ± 600	248.3 ± 0.4	11.1 ± 1.2	3.49 ± 0.03
	-208200 ± 600	248.1 ± 0.4	9.9 ± 0.6	3.65 ± 0.01
ii[a]	-295300 ± 600	272.6 ± 0.4	14.0 ± 0.6	6.02 ± 0.01
	-294800 ± 600	272.5 ± 0.5	14.0 ± 0.4	6.51 ± 0.01
iii[a]	-414700 ± 600	299.2 ± 0.5	16.2 ± 0.7	9.77 ± 0.03
	-414700 ± 800	299.5 ± 0.5	16.5 ± 0.4	9.00 ± 0.07

[a] In the parallel runs, only the random seeds in building the initial structures are different. Three parallel simulations are performed for mixture i, which has the slowest dynamics of water. [b] Dielectric constant of waters. Error estimates are determined by block averages of 20 ns in length. The experimental value of ϵ is less than 19 in PSS/PDADMA PEMs.[8,60] For pure waters system, the experimental value of ϵ is 78.3,[58] and $\epsilon = 71 \pm 6$ for the SPC/E water model.[59] [c] Unit: 10^{-7} cm^2/s. Determined from the mean-square-displacement data in the time range of 20 - 50 ns, in which the diffusion is approximately obtained. For bulk SPC/E water system, our calculated diffusion coefficient is 2.6×10^{-5} cm^2/s at ambient condition.

III. Results and Discussion

A. Validation of the Obtained Trajectories. The electrostatic interactions present in our systems pose a severe hindrance for numerical simulations to get proper equilibrated systems. In order to ensure that the equilibrium state has been reached, the fluctuations of the energy and the volume have been monitored during the production runs for several different initial conditions, see Table 2. In addition, the dielectric constant and the diffusion coefficient of the water molecules have been also computed. The error bars next to the averaged values depict the standard deviations registered during the 100 ns. Results in Table 2 support the idea that production runs are performed in the equilibrium state of the systems.

Further checks have been performed in order to ensure the independence of the results on the initial conditions: system i has the biggest PE concentration (~2.82 mol/L in monomer unit) and is thus expected to show the slowest dynamics. Therefore, for such system we have done three runs with different initial conditions. For lower PE concentrations, systems ii and iii, two simulations with different initial conditions have been performed. The initial structures are built up using Packmol with different random seeds. The same simulation protocol has been applied to all of them. The dielectric constant and the diffusion coefficient are dynamic properties which take a long time to be estimated accurately and therefore can help us as an extra benchmark of the quality of our equilibration protocol. Results for the dynamical properties of water are listed in Table 2. The results show a coherent agreement, which supports that the equilibration protocol is suitable to obtain an equilibrium state in the simulated systems. The large fluctuations observed for the water diffusion coefficient will be discussed later in section III.D.

The statistical analysis of the static properties has been done using the results of the first run for each system because differences for those observables among the different runs for the same system are very small. For instance, the coordination number of sulfur around nitrogen is calculated to be 2.39, 2.32, and 2.36 in the three different simulations for system i, which gives a deviation of less than 3%. However, for the statistical analysis of the dynamical properties, all the simulations available for a same system are averaged due to the relatively larger fluctuations of such observables.

B. Ion-Pairing. Both PSS and PDADMA are known to be strong PEs and to lead to the formation of PEMs dominated by electrostatic interactions.[45] In such type of PEMs, the charge reversal (overcompensation), which is originated from the charged adsorbing substrate, is assumed to play an important role during PEM formation. The ratio between the mixing enthalpy ΔH and Gibbs free energy ΔG has been observed to be $\Delta H/\Delta G \approx 0.57$ for such PEMs.[45] Therefore, an investigation on the ion-pair formation, mainly due to the electrostatic interaction, is critical to understand the buildup of PSS/PDADMA PEMs. Initially, it was assumed that the salt ions are completely expelled out of the PEMs. In that scenario, all the charge groups on polycations are charge compensated by the oppositely charged polyanions, which is called an intrinsic charge compensation mechanism. Experiments have shown strong evidence for the intrinsic charge compensation scenario to be unrealistic (see for example, refs 28, 46, and 47). A more realistic situation for PSS/PDADMA PEMs corresponds to the case where charge groups of PEs are compensated by salt ions of opposite charge (extrinsic compensation mechanism). Despite of the rinsing stages performed in the building up of PEMs, salt ions have been observed to remain within the PEMs: Schlenoff et al. have found that the salt ions cannot be completely expelled out of the PSS/PDADMA PEMs even though the PEMs are surrounded by a water buffer region containing no salt.[28]

Current experiments allow to roughly estimate the approximate amount of salt present in the PEMs under extremely dilute salt concentration in the water buffer region.[28] Unfortunately, with the current experimental state of the art, it is not possible to obtain detailed information related to the electrostatic pairings of PE−PE and PE−counterion. A knowledge about the ion distribution inside the PEMs and the relative strength of the electrostatic pairings may help to develop more elaborated theoretical and numerical models, and in turn it may provide useful information to tune the properties of PEMs. One of the main goals of this paper is to provide a first hint about the electrostatic pairing in the inner layers of PEMs via the study of the PEs/water/salt mixtures.

It is noteworthy that due to the homogeneous nature of the systems investigated here, the influence of the substrate effect in PEM formation and the interfacial region between PEM and the water buffer region cannot be studied. Also, since the symmetric PEs (in chain length, charge ratio and concentration) are used here and our systems are charge neutral, the charge reversal is not expected to occur in the present work. In real PEM systems, the entropic effect as well as the presence of a water buffer region are expected to play significant roles, and thus the ion-pairing in the inner layers of PEMs may change significantly. For instance, the probability of the extrinsic charge compensating of sulfonate groups from PSS in system i is calculated to be about 10% (see Figure 3), bigger than the experimental average of 6%.

1. PE−PE vs PE−Counterion. In the following text, S refers to the sulfur atoms on PSS, and N stands for the nitrogen atoms on PDADMA. They are used to represent the charge groups on PSS and PDADMA (i.e., $[CSO_3]^-$ and $[CH_2CH_3\text{-}CH_3CH_2)N]^+$, respectively (see Figure 1). Such selection is done because those atoms are close to the geometrical center of the groups. The radial distribution functions (RDFs) between the oppositely charged atoms are depicted in Figure S2 of the Supporting Information. Figure S2 shows that the first minimum of the S−N RDF shows a very weak dependence on the salt concentration: it remains at a rough distance of 0.64 nm for all mixtures under study. Therefore, in the following $r_c = 0.64$ nm is taken as the cutoff distance for the ion-pair formation with an except of Na−Cl ion-pairing.

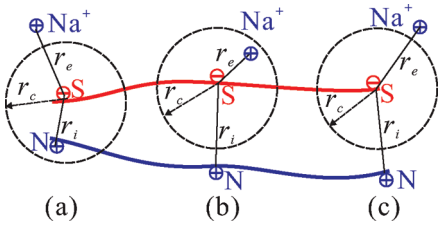

Figure 2. Schematic representation of the definitions of intrinsic and extrinsic charge compensation used in the present work. S, and N stands for the sulfur atom on PSS and the nitrogen atom on PDADMA, respectively. Take sulfur as the reference, r_i is the distance to the nearest nitrogen, and r_e is the distance to the nearest Na^+. r_c = 0.64 nm is the cutoff distance of the first S−N coordination shell. When (a) $r_i < r_e$ and $r_i < r_c$, the sulfur is intrinsically charge compensated; (b) $r_e < r_i$ and $r_e < r_c$ represents the fact that sulfur is extrinsically charge compensated; (c) $r_i > r_c$ and $r_e > r_c$ means the sulfur is noncompensated.

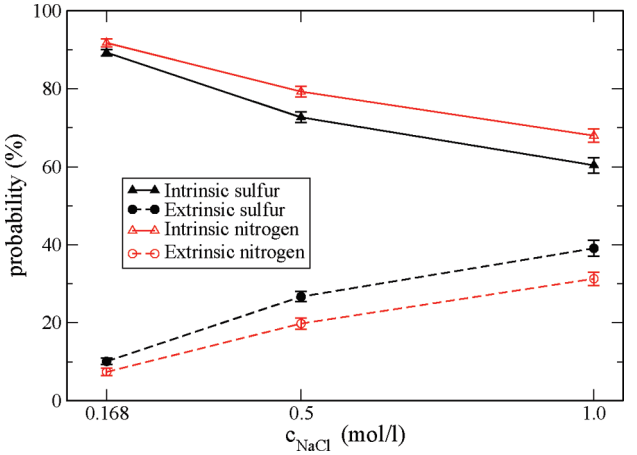

Figure 3. Probabilities of sulfurs and nitrogens which are intrinsically and extrinsically charge compensated. See Figure 2 for their definitions. The error bar is the standard deviation.

In order to study the relative weight of the different types of charge compensation (intrinsic and extrinsic) inside the mixture, one must first define a criteria for the different groups: we assume that every charged PE group can be compensated only via a single oppositely charged PE group or salt ion; we consider a sulfonate (ammonium) to have no pair if the closest distance r to an ammonium or Na^+ ion (sulfonate or Cl^- ion) is larger than $r > r_c$. Otherwise the sulfonate or ammonium are said to be "charge compensated" or to form an electrostatic pair. We consider the pair to be of intrinsic nature if the sulfonate (ammonium) group has an ammonium (sulfonate) group which is located closer to it than any Na^+ (Cl^-), otherwise it will be extrinsically compensated according to our definition. Figure 2 shows a pictorial representation of our used criteria.

Figure 3 shows the probabilities of the intrinsic and extrinsic charge compensation of the PSS and PDADMA groups. The contribution arising from noncompensated PE charge groups, which originate from the hydration behavior, is always below 1% of the groups, and therefore will be neglected in what follows. For system i, the PE charge groups intrinsically charge compensated account for about 90% of the total, whereas only ca. 10% are extrinsically charge compensated. These results clearly support that the intrinsic charge compensation mechanism dominates over the extrinsic mechanism in PSS/PDADMA systems. As expected, with the increase of the salt concentration, the intrinsic charge compensation becomes less dominated (passing from about 90% to about 60−70%).

It should be remarked that in system i, the charge compensation contribution due to Na^+ ions, (ca. 10% of the total cases), is much larger than the molar ratio of Na^+ to sulfur, namely 0.06. This can be explained as a consequence of the fact that the S−Na interaction is stronger than the S−N interaction. A further proof of the interaction difference will be presented later when discussing the calculation of the interaction energies between the different charge groups. Similar conclusions can be obtained in the study of system ii, but not in system iii, the difference is assumed to be related to the Na−Cl ion-pair formation discussed in the next section.

Figure 3 also shows that the probability of extrinsic charge compensation of PSS charged groups (10%) is larger than that in the case of PDADMA charge groups (7%). Given that both groups have also the chance to form S−N ion-pairs, it is reasonable to conclude that the S−Na interaction is stronger than the N−Cl interaction.

A further proof about the strength of the different electrostatic pairs is provided by the measurement of the nonbonded (coulomb and LJ potential) energies which are calculated based on the ion-pairing: if the central atoms of two oppositely charged groups are within their first coordination shell, they are considered as being bound. The first coordination shell is defined as the first minimum on the corresponding RDF curve (see Figure S2 in the Supporting Information). The bounding energy is calculated on all the atoms distributed on these two charge groups. For PSS, the center atom of the charge group $[CSO_3]^-$ is chosen as sulfur, and for PDADMA, nitrogen from $[CH_2CH_3CH_3CH_2)N]^+$. The obtained interaction energy per ion-pair (in kJ/mol) follows the order: Na−Cl (−520 ± 20) > PSS−Na (−420 ± 20) > PDADMA−Cl (−280 ± 30) ≅ PSS−PDADMA (−270 ± 20), which is in good agreement with the previous results. On the other hand, the energy calculation also shows that the LJ interactions (E_{LJ} = −10−20 kJ/mol) can be ignored in comparison with the Coulomb interaction. The interaction energies between the different ion-pairs are collected in Table [S1] in the Supporting Information.

We define the coordination number as

$$N(r_c) = 4\pi\rho \int_0^{r_c} g(r) r^2 \, dr \qquad (1)$$

where $g(r)$ is the RDF, and ρ is the number density. The coordination number $N(r_c)$ can provide additional information on the ion-pairing. Figure 4 shows the coordination numbers calculated using a cutoff r_c = 0.64 nm, for the nitrogen around sulfur(or S around N equally), Na^+ around sulfur and Cl^- around nitrogen. When the salt concentration increases (c_{NaCl} = 0.168, 0.5, 1.0 mol/L), the coordination number of S around N (or N around S equivalently) decreases from 2.4 to 2.1 to 1.9. This can be explained due to a 2-fold effect of the salt increase: the PEC structure is becoming looser ($c_{monomer}$ decreases from 2.8 to 2.6 to 2.3 mol/L), and the electrostatic screening is becoming stronger.

In the very short distance region, the higher cumulative number of Na^+, compared with that of N atoms, around S atoms is apparently due to the relatively smaller steric hindrance of Na^+. Up to the cutoff distance of 0.64 nm, there are about 0.18 Na^+ distributed around every sulfur atom in system i. Given that the overall molar ratio of Na^+ to sulfonate groups is 0.06 in this mixture, it is suggested that every Na^+ is shared by about 3 sulfur atoms, which can be verified using the calculated coordination number of sulfur

atoms around Na^+: 3.0, 2.8, and 2.3 for systems i−iii, respectively. In a similar way, the coordination number of nitrogen atoms around Cl^- is found to be 2.6, 2.3, and 1.8, respectively.

Figure 4, shows that the coordination number of Na^+ around sulfur is always larger than that of Cl^- around nitrogen. The difference between these two cases is consistent with the previous calculation of the nonbonded energies between ion-pairs.

Figure 5 shows, for system i, the 3-dimensional spatial distributions of salt ions and PE charge groups around an opposite charged PE group. In that representation the coordinates of sulfur and nitrogen atoms are taken as the origin point, i.e., (0,0,0). Panel a shows that the distribution of Na^+ around sulfur has a biased orientation in the direction along the S−O···Na^+ bond. On the other hand, nitrogens occupy mainly the regions above and below the benzene ring, and above the sulfonate group. The stacking of the PSS and PDADMA rings, as shown in panel c, is an expected feature arising from the aromatic nature of the cycles. Nonetheless, panel c also shows that the orientation between the rings of PSS and PDADMA disappears very quickly. On the other hand, due to the large steric hindrance of $-CH_2-$ and $-CH_3$ around the Nitrogen atom on PDADMA, there is no well-defined orientation of sulfur and chloride around it, and the occurrence of chloride around nitrogen is so small that its isosurface overlaps with that of sulfur, as shown in panel b.

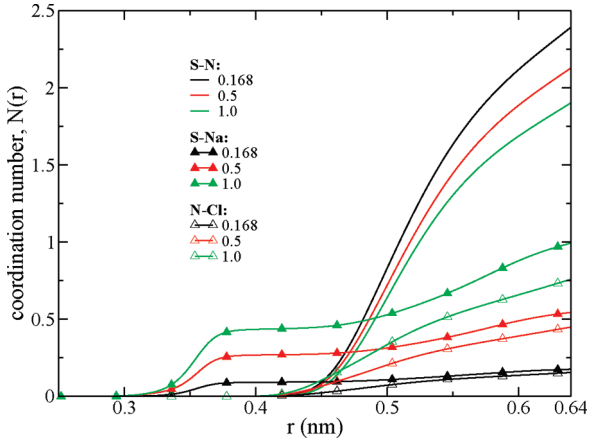

Figure 4. Effect of NaCl concentration on the coordination number of N around S (or S around N equally) (lines), Na^+ around S (lines with solid triangles), and Cl^- around N (lines with empty triangles). S and N represents the sulfur atom on PSS and nitrogen atom on PDADMA, respectively. 0.64 nm is the cutoff distance of the first S−N coordination shell.

2. Na−Cl. Taking into account that the Na−Cl ion-pair has the largest interaction energy, one may conclude that the ion-pairing between them is strong. In order to test that idea, the coordination number of chloride around sodium is calculated. The cutoff distance we take in eq 1 is the first minimum of the Na−Cl RDF, i.e., r_c = 0.35 nm. The coordination numbers obtained are as follows: 0.05, 0.15, and 0.40 for systems i−iii, respectively, which shows that the previous idea only holds in systems with a high concentration of salt. The low probability of Na−Cl ion-pair formation in system i is attributed to the fact that the salt ions are charge saturated by several (3 for Na^+ and 2.6 for Cl^-) oppositely charged PE groups. The structure formed by salt ions and the surrounding polyions is stable enough with regard to the potential energy, whereas the presence of more water facilitates the Na−Cl ion-pair formation in system iii.

C. Hydration Behavior. The hydration ability of PEs (see, e.g., refs 28 and 47), as well as the water distribution inside PEMs,[48−50] has not been studied in detail despite the fact that those factors have a great impacts on the mechanical properties and the applications (e.g., membranes) of PEMs. The PEMs composed of different PEs show strong differences in their hydration behavior.[47] Furthermore, several studies have related the odd−even effect in the thickness of PSS/PDADMA PEMs to hydration ability and also in part to the effect of the substrate. The odd−even effect consist in an alternating PEM shrinking and swelling depending

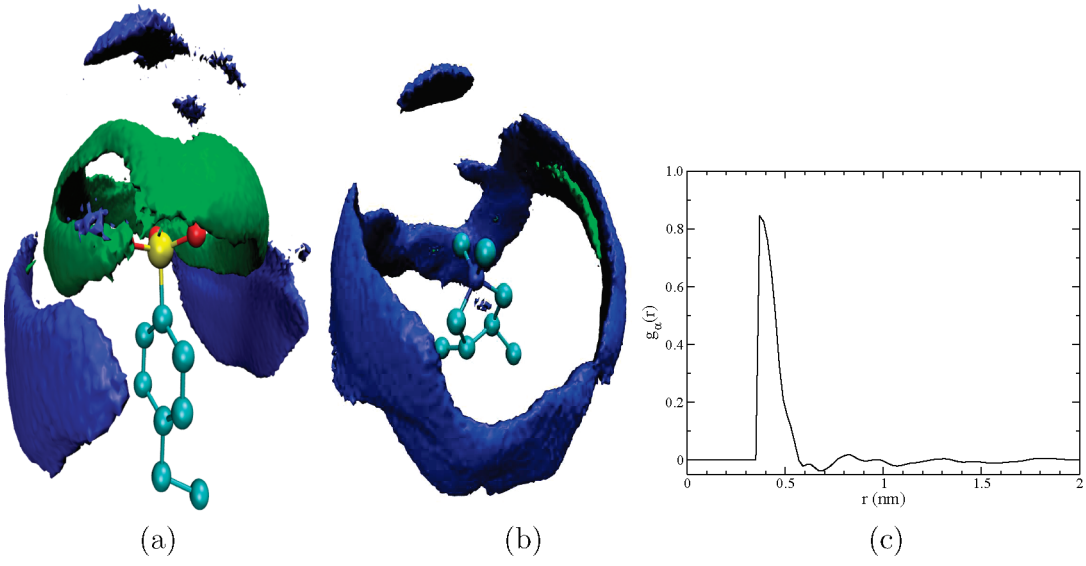

Figure 5. 3-dimensional spatial distribution in mixture i) of (a) nitrogen (in blue) and Na^+ (in green) around sulfur on PSS, and b sulfur (in blue) and Cl^- (in green) around nitrogen on PDADMA. A distance range of $r \leq 0.64$ nm from the coordinates of S (panel a) and N (panel (b)) is considered. The isosurfaces in blue and green are plotted at the number density of 0.01 $Å^{-3}$ and 0.002 $Å^{-3}$, respectively. The hydrogen atoms are not shown. Panels a and b are generated using VMD. (c) Stacked orientation between the rings of PSS and PDADMA in mixture i. $g_\alpha(r) = (1/N(r))\sum_{i,j}[{}^1/_2(3\cos^2(\alpha_{ij}(r)) - 1)]$, where i and j refer to the ith ring of PSS and the jth ring of PDADMA, r is the distance between the geometry centers of the ith and the jth rings, $\alpha_{ij}(r)$ is the angle between the normal vectors of the ith and the jth ring at the distance of r, and $N(r)$ is the total number of neighbor rings at the distance of r. $g_\alpha(r) = 1$ means that the rings of PSSs are parallel to those of PDADMAs, and 0 stands for random orientations.

Table 3. Some Calculated Coordination Numbers[a]

mixture	S−O	N−O	Na−O	Cl−O	O−O[b]
i	13.9	14.3	17.3	18.9	2.7
ii	15.4	16.0	19.2	20.4	2.9
iii	16.2	16.4	22.2	22.7	3.1

[a] Coordination number of the water oxygen around sulfur, nitrogen, Na, Cl and water oxygen. S, N, and O represent sulfurs on PSSs, nitrogens on PDADMAs and water oxygens, respectively. r_c = 0.64 nm in eq 1 for all except O−O. [b] r_c = 0.33 nm in eq 1. The coordination number of waters around water is 4.3 in our pure SPC/E water system at ambient condition.

whether the number of deposited layers is odd or even (see, for example, ref.[8]). Schlenoff and co-workers[28] have reported that PSS/PDADMA PEM swell with PDADMA deposited as the topmost of an odd layer. Furthermore, they have suggested that PDADMA in the outermost layer (compensated by Cl^-) has a stronger hydration ability than PSS (compensated by Na^+ in the outermost layer).

1. Ion−Water. Table 3 shows the coordination numbers of waters around sulfurs, nitrogens, sodiums and chlorides calculated using a cutoff distance r_c = 0.64 nm. Such coordination numbers give us insight about the hydration ability of the different PE charge groups and salt ions. The results in Table 3 show that water coordination numbers for all species increase with the salt concentrations due to the fact that more water is present in the system, and salt ions show a higher affinity for water molecules. The larger affinity of the salt ions can be explained as a consequence of the fact that PEs have hydrophobic backbones.

The difference between the values of the coordination number of waters around PDADMA (compensated by Cl^-) and around PSS (compensated by Na^+) can be split in a contribution arising from the environment surrounding PEs, and a second contribution arising from the environment surrounding the salt ions. It should be noticed that the contribution of salt ions should be rescaled by the molar ratio of salt ions to PE charge groups. Taking results from Table 3, the contribution due to the PE can be calculated to be 0.4, 0.6, and 0.2 for systems i−iii, respectively. The second contribution arising from salt ions is 0.1, 0.2, and 0.2 for each one of the three systems. Thus, the total coordination number of waters around the ionic pair PDADMA−Cl^- are larger (i.e., 0.5, 0.8, and 0.4) than those for the PSS−Na^+ pair. These findings are consistent with Schlenoff,[28] although the differences are quite small when compared with the total coordination number of waters around the different species. This behavior could explain why the odd−even effects becomes very weak after the substrate effect disappears (more than 10 bilayers) as it can be observed in Figure 2 of ref 28. Therefore, one can infer that the strong odd−even effect occurring in the first few PSS/PDADMA PEM layers is due to the substrate effect and not to the PE hydration behavior. Nonetheless, the influence of the substrate effect cannot be studied in our work due to the homogeneous nature of the systems we are studying, and will be left to subsequent study.

Experimentally, it has been reported that the hydration number of sodium is bigger than that of chloride (see Table 3 in ref 28 or the original reference[51]). This is apparently in contradiction with our results. In order to explain the differences between experiments and our numerical simulations, one should keep in mind that by definition, the hydration number is the number of water molecules that remain associated with the ion during its movement, while the coordination number is defined as the total number of waters which are in contact with the ion.[51] Thus, the coordination number is a static quantity, while the hydration number is a kinetic property. The hydration number is generally smaller than the coordination number, even though they tend to be identical for very small ions. As the size of the ion increases, a larger difference can be expected between the hydratation number and the coordination number. On the other hand, our results agree with other numerical simulations for NaCl in aqueous solution at ambient condition[52] when one compares the positions of the first maxima and minima in the Na−O and Cl−O RDFs, as well as the trend of the coordination numbers of waters around Na and Cl (see Figure 3 in ref 52 and Figure S3 in the Supporting Information in this work).

Another point to take into account when describing the hydration ability in terms of the water coordination and hydration number is the difference in volume between the ions $[CSO_3]^-$ and $[N(CH_2CH_3)_2]^+$, the latter of which has a larger volume. Despite the fact that nitrogen has a bigger coordination number of waters, it is not possible to predict a larger hydration number for nitrogen. Thus, one must be careful about which concept, either hydratation or coordination number, is addressed when describing the hydration ability of the ion pairs. Experimentally, the coordination number can be obtained from X-ray measurements, whereas ultrasonic velocity measurements are used in order to determine the hydration number.[51] The swelling behavior of PEMs is related to the coordination number of water and not to the hydration number because the coordination number has a thermodynamic nature.

Table 3 also shows the behavior of the coordination number of waters around waters as a function of the salt concentration. The increase of such coordination numbers with the increase of salt concentration is a consequence of the fact that more water molecules are present in the systems with more salt ions. Nonetheless, in all tested systems, the coordination numbers of water around waters is far below the saturation value of 4.3. Such saturation value has been obtained from a pure water simulation containing 4000 SPC/E water molecules that has been run for 20 ns.

2. Porosity. The mean size of pores in PEMs due to the presence of water molecules can be experimentally determined using NMR cryoporometry[50] and permeation experiments.[48,49] Experiments made on PSS/PDADMA[49] and PSS/PAH[48−50] PEMs show that typical values for pore sizes are close to 1 nm. The NMR cryoporometry determines the average size of the water-filled pores while the permeation experiments measure the sizes of those paths over which the waters are interconnected. Both experimental techniques report similar pore sizes and therefore one can conclude that water inside PEMs forms a homogeneous nanostructure.[8]

Atomistic simulations can provide a further insight on the details of such water nanostructure inside PEMs because in difference to experiments one knows with precision the position and orientation of all molecules and atoms present in the system. In order to characterize such water structures, one has to resort to a definition of what constitutes a water cluster inside a PE mixture. Hereby, a water cluster is defined as follows: a water cluster is composed of a cluster core and a cluster shell: those water which have no neighbor of any PE atoms are forming the cluster core; based on the formed cluster core, those waters which have both neighbors of waters belonging to cluster core and PE atoms are labeled as cluster shell. The cutoff distance of the first O−O coordination shell (i.e., 0.33 nm) is chosen as the distance criteria for the neighbor calculations, in which O is the oxygen of water. The definition of a water cluster allows us to estimate the probability (expressed in %) that a water

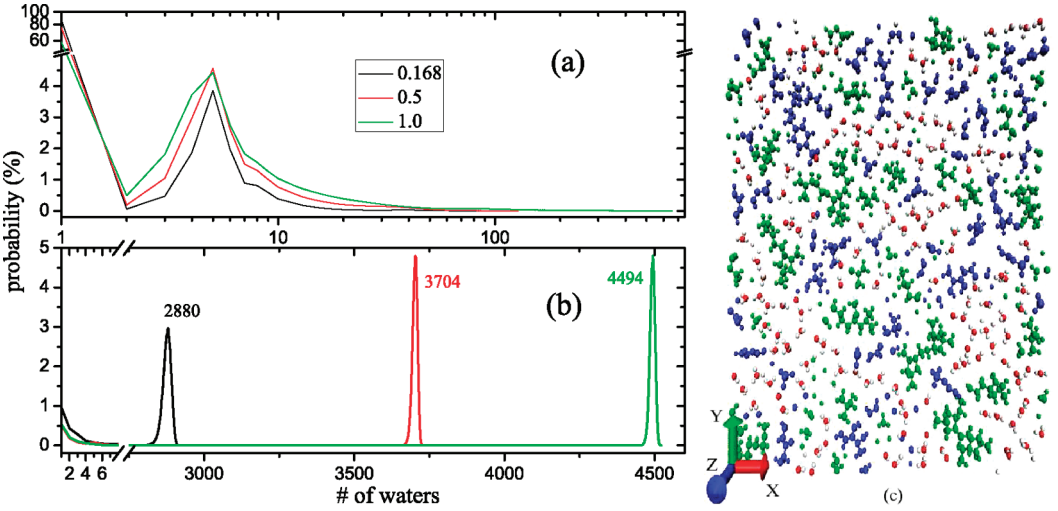

Figure 6. Effect of salt concentration on the probability (eq 2) of how many waters are (a) clustered, and (b) connected to each other. The distance criteria is chosen to be $r \leq 0.33$ nm (the first O−O coordination shell). In panel a, a cluster is composed of two parts: cluster core and cluster shell. The former refers to those waters which have no neighbor of PE atoms; and the later is formed by those waters which have both neighbors of cluster core waters and PE atoms. In all the three mixtures, the water clusters of the biggest probability include 5 water molecules, and most of the waters (≥59%) are not clustered. In panel b, if only the distance between two water oxygens satisfies the distance criteria, they are considered to be connected. In the three systems, 2880, 3704, and 4494 waters of the biggest probability are connected to each other, which stands for 98.0%, 99.1%, and 99.1% waters of the corresponding systems. (c) Distribution of waters with the surrounding polyelectrolyte atoms, as generated from the last frame of mixture i by VMD. PSSs are in blue, PDADMAs are in green, and water oxygen/hydrogen are in red/white, respectively. Salt ions are not shown. Only a slap of the thickness of 0.33 nm is shown ($X = Y = 6.27$ and 2 nm $< Z \leq 2.33$ nm). The waters show a network-like distribution.

molecule is found inside a cluster of waters with a core size i (namely, number of waters inside):

$$\text{probability}(i) = 100 \times \frac{i \times \sum_{frames} n(i)}{\sum_{frames} N} \qquad (2)$$

where $n(i)$ is the number of clusters having a core size i, and N is the total number of waters in the system.

Figure 6a shows probability(i) as a function of the water cluster core size i. Clusters with a core size $i = 5$ are found to be the most probable ones. The volume of a typical cluster can be roughly estimated using the bulk water density $\rho = 1$ g/cm^3 and is found to be 0.15 nm^3. Such value for the cluster volume is slightly smaller than the mean volume of the pores that have been experimentally determined. Chavez et al.[50] have found that if one assumes the pores to have a spherical shape, a pore with a rough diameter of 1 nm has a mean volume close to 0.5 nm^3. The difference between the numerical and the experimental values can be reasoned as follows: the definition of porosity used by us is different from the one used in the experiments where PE atoms might have been taken into account which undoubtedly will result in bigger pore sizes; on the other hand, in experiments using freshly prepared PEMs the amount of water inside the multilayer can be larger than the value one would found in an equilibrium situation (it is reported that the initial water content decreases until reaching a plateau at equilibrium[28]).

Figure 6 also shows that the maximum core cluster size increases from less than 100 to more than 600 when the salt concentration is increased. This behavior can be explained in terms of a larger absorption of waters and the increasing probability of Na−Cl ion-pairing. Notice that most of the waters (86%, 76% and 59% for systems i−iii, respectively) are not clustered (cluster size equal to 1), which can be due to either only the cluster core of size of 1 is formed (i.e., the waters are completely surrounded by salt atoms) or no cluster core is formed for such waters. To further investigate the distribution of the waters, another observable is defined: the connectivity between waters. Two waters are said to be connected if the distance between their oxygen atoms is less than 0.33 nm, one can then analyze how many waters are connected. Figure 6b shows the calculated results. System i shows a peak for connected structures of 2880 waters, such structures represent 98.0% of the total number of waters in the system. For systems (ii) and (iii), the size of the most probable connected structures gathers 99.1% and 99.1%, respectively, of the total amount of waters. The average number of unconnected waters represents ≤2% of the total, and it corresponds to waters which are completely surrounded by PE atoms and/or salt ions within the distance range of 0.33 nm.

Parts a and b of Figure 6 show that the probability of water cluster formation is very low and that most of waters are in average distributed in a network-like form having links one with the others. The previous results are coherent with the homogeneous water distribution prediction done by Schonhoff et al.[8] based on their experimental results. Figures 6c shows a snapshot of a slab with a thickness 0.33 nm generated from the last recorded conformation of system i, where only the waters and the surrounding PE atoms are depicted. The snapshot gives a clear idea of the network-like distribution of waters inside the mixture.

D. Slow Dynamics of Waters. The slow dynamics of waters in PEMs has been experimentally studied,[53] but no theoretical or numerical works have been devoted to the issue. Some recent simulation studies[54−56] have provided an important insight about the dielectric constant of waters in concentrated electrolyte solutions where electrostatic interactions can be almost twice as strong as in pure water. Since waters can be expelled out of PEMs during its buildup, one expects an enhanced electrostatic interaction. A signature of such strong Coulomb interactions inside the PEMs is the slow dynamics for water molecules inside PEMs due to electrostriction. The slow dynamics of waters inside PEMs can be basically monitored via the study of the static dielectric

constant (i.e., static relative permittivity) and the water diffusion coefficient.

1. Dielectric Constant. The dielectric constant, ϵ, depends on the average of the total dipole moment of the system $\vec{M} = \sum \vec{\mu}_i$, and it is calculated according to[57] as:

$$\epsilon = 1 + \frac{1}{3Vk_B T\epsilon_0}(\langle \vec{M}^2 \rangle - \langle \vec{M} \rangle^2) \quad (3)$$

where V is the volume, T is the temperature of the system, and ϵ_0 denotes the dielectric constant of vacuum. The experimental dielectric constant of pure water at ambient condition is 78.3,[58] and the dielectric constant reported for SPC/E water model is 71 ± 6.[59]

Table 2 shows the dielectric constants of waters for our three different systems. All the values fall into the range 9.3−16.9, and an increase of the dielectric constant is observed with increasing salt concentration. The increase here is due to the fact that with increase of salt also the amount of water inside the PEMs increases, which reduces the electrostriction of water. Experimentally, it has been predicted that the dielectric constant of PSS/PDADMA PEMs should be smaller than 19.[8,60] Our calculated results are in good agreement with the experimental data. Moreover, the buildup of PEMs is generally performed at salt concentration of less than 1 mol/L, and PSS/PDADMA PEMs have been reported to be stable at the salt concentration smaller than 2 mol/L.[6]

Our results show that the dielectric constant of water in the PE mixtures under study are greatly reduced when compared to the values observed in pure water systems. This result clearly supports also the idea that water inside PSS/PDADMA PE mixtures exhibits a slow dynamics: the slower the dynamics is, the larger is the water ordered, and consequently, the lower is its dielectric constant.

So far, in the coarse-grained models used to study PEMs, an homogeneous dielectric background is assumed for the interior and exterior of the PEMs. This approximation apparently underestimate the Coulomb interaction inside PEMs. In ref 10, the idea of space-dependent dielectric constant was already proposed. The present results give further support to the idea that coarse-grained simulations of PEMs must be further refined.

2. Diffusive Behavior of Waters. The diffusive behavior of a particle can be classified according to the exponent β governing the temporal evolution of the mean-square-displacement

$$\langle |\vec{r}(t) - \vec{r}(0)|^2 \rangle = \Delta r^2 \propto \Delta t^\beta \quad (4)$$

A value of $\beta = 1$ is associated with a random diffusive behavior of the particle, which is the regime generally used to determine transport properties like the diffusion coefficient. In systems where electrostatic interactions govern the dynamics of the system, particles remain for long times trapped into local cages formed by surrounding particles which leads to temporal exponents $\beta < 1$. In such Coulombic systems, the random diffusion regime is only achieved for very long simulation duration.[61] On the other hand, at very short times, in the subpicosecond regime, particles tend to move following straight paths. Such regime is know as the ballistic regime and is characterized by a temporal exponent $\beta = 2$.

An accurate determination of the diffusion coefficient of water can only be done by ensuring that time intervals taken into account fall within the random diffusive regime. Figure 7 shows the temporal evolution of the exponent β for different species in system i, which is the one expected to have the slowest dynamics due to its high concentration of PEs. Because of the poor statistics for large Δt, values of β are only shown for $\Delta t < 60$ ns. Clearly, only water molecules are able to reach the random diffusive regime within the time framework of our simulations, one can roughly consider water molecules to be in such regime when $\Delta t > 20$ ns. PEs and salt ions would need longer simulation times in order to be able to characterize properly their diffusive behavior.

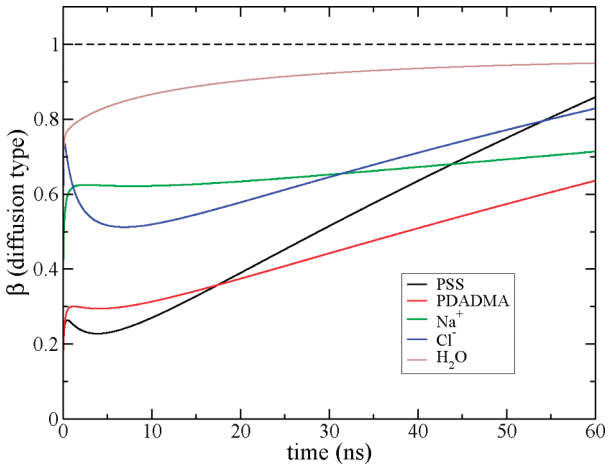

Figure 7. Temporal evolution of the diffusion exponent β for several species in system i, (see eq 4). The horizontal dash line with $\beta = 1$ represents the random diffusion behavior. For $\beta < 1$, the particles are trapped in local cages formed by surrounding particles. The value of β is obtained from the fitted function of $f(x) = \sum_{i=0}^{5} A_i x^i$ to the original data of $\log(\Delta r^2) \sim \log(t)$ in the time range 0−60 ns.

The diffusion coefficient of waters is obtained within the random diffusive regime ($\Delta t \in [20, 50]$ ns) using the common expression

$$D = \frac{\Delta r^2}{6t}$$

Table 2 on the last column shows the water diffusion coefficients obtained for each mixture and run. Water diffusion coefficients are in the range (3.5−9.8) × 10^{-7} cm^2/s, and as expected, with the increase of the salt concentration (which implies a lower density of PE) the water diffusion coefficients increase. It is noteworthy that the obtained results for the diffusion coefficient of water are in good agreement with the experimental ones, which were measured to be about 2 × 10^{-7} cm^2/s by pulsed field gradient diffusion NMR.[62] For pure water, the SPC/E water model predicts a water diffusion coefficient of 2.6 × 10^{-5} cm^2/s, and therefor one can conclude that in the PE mixtures under study the water molecules diffuse roughly 2 orders of magnitude slower than in pure water. Therefore, the results of the water diffusion inside our PE mixtures lead to the same conclusion as our dielectric measurements: water molecules inside PE mixtures exhibit a slow dynamics when compared to water molecules in a bulk environment.

IV. Conclusions

Extensive explicit solvent AA MD simulations of PSS−PDADMA polyelectrolyte mixtures have been performed. Several systems containing salt (NaCl) and water concentrations close to those found experimentally inside polyelectrolyte multilayers are studied in detail. Increasing the salt concentration from 0.168 up to 1 mol/L we find that the PE mixture swells. We observe that the intrinsic charge compensation dominates in all investigated systems, but its relative weight decreases from about 90% to about 60%. On the other hand, the interaction energy per ion-pair follows the order: Na−Cl > PSS−Na > PDADMA−Cl ≅ PSS−PDADMA, that is, the extrinsic charge compensation is

expected to be preferred energetically (in particular for PSS). These facts indicate that the interaction energy does not play an exclusively role in the ion-pair formation, and to precisely understand the ion-pairing in real PSS/PDADMA PEMs, the entropy effect should be taken into account. Moreover, for PSS/PDADMA/NaCl solutions, sodium is expected to be found in higher concentration than chloride inside PEMs. When the NaCl concentration is low, salt ions are found to be charge saturated by up to three oppositely charged PE groups.

Our simulational results agree with the experimental findings for PDADMA−Cl pairs that show a stronger hydration behavior than for PSS−Na pairs. However, the observed difference is so small that we are lead to conclude that this difference should not play any significant role in the experimentally observed odd−even effect for the PEM buildup. Instead, we believe that the presence of a substrate is responsible for the odd−even effect, which is presently under investigation.

The water analysis suggests that the distribution of waters are network-like and homogeneous, which is in agreement with the experimental results. Water molecules inside our mixtures are strongly bound and exhibit a slow dynamics within the PE mixtures. This behavior can be inferred from the measurements of the dielectric constant and the diffusion coefficient of water. The measured dielectric constants in the PE mixtures are in the range $\epsilon \in [9.3, 16.9]$, i.e., roughly 1 order of magnitude smaller than that for pure water. The measured diffusion constants for water inside the PE mixtures are 2 orders of magnitude lower than for pure water. If the salt content is reduced the dynamics of water molecules slows down even further.

Although present computer capabilites limit our study to mixtures of short chains with polymerization degree up to DP = 12, we were nevertheless able to show that basic physical properties of the PE mixture are very similar when chains with DP = 12 or DP ≥ 3 are, which is consistent with a very recent experimental study on strongly charged PAA/PDMAEMA PECs. Thus, we conclude that the performed simulations are able to provide some useful insight for forthcoming theoretical and experimental works. We also hope that our results can be useful for refining present coarse-grained (CG) models or to develop hybrid models that combine AA/CG ideas. We believe that to accurately tackle PEM systems, a high resolution model of PEs and solvents is necessarily required in the region close to the substrate, although such condition could be relaxed in the water buffer region.

Acknowledgment. B.Q. and C.H. want to acknowledge support through the SPP 1369 and a DFG grant HO 1108/12-1. J.J.C. expresses thanks for the financial support of Spanish Ministerio de Educación y Ciencia, Postdoctoral Grant No. EXP2006-0931. B.Q. also thanks HLRS for using the bwGRID computer resources.

Supporting Information Available: Text giving the formulation of the OPLS-AA force field potential, figures showing RDFs of PSS/K^+ /H_2O system and the comparison with previously reported RDFs and RDFs between oppositely charged groups/atoms; coordination number of waters around sulfur from PSS, N from PDADMA, Na^+, Cl^-, and waters of mixtures (i), and a table of nonbonded energies per ion-pair between oppositely charged PEs and salt ions. This material is available free of charge via the Internet at http://pubs.acs.org.

References and Notes

(1) Schmitt, J.; Decher, G.; Hong, G. *Thin Solid Films* **1992**, *210/211*, 831.
(2) Decher, G. *Science* **1997**, *277*, 1232–1237.
(3) Schlenoff, J. B. *Langmuir* **2009**, *25*, 14007–14010.
(4) Schönhoff, M. *Curr. Opin. Colloid Interface Sci.* **2003**, *8*, 86–95.
(5) Schönhoff, M. *J. Phys.: Condens. Matter* **2003**, *15*, R1781–R1808.
(6) von Klitzing, R.; Wong, J.; Jäger, W.; Steitz, R. *Curr. Opin. Colloid Interface Sci.* **2004**, *9*, 158–162.
(7) von Klitzing, R. *Phys. Chem. Chem. Phys.* **2006**, *8*, 5012–5033.
(8) Schönhoff, M.; Ball, V.; Bausch, A. R.; Dejugnat, C.; Delorme, N.; Glinel, K.; von Klitzing, R.; Steitz, R. *Colloids Surf., A* **2007**, *303*, 14–29.
(9) Dobrynin, A. V. *Curr. Opin. Colloid Interface Sci.* **2008**, *13*, 376–388.
(10) Cerdá, J. J.; Qiao, B.; Holm, C. *Soft Matter* **2009**, *5*, 4412–4425.
(11) Cerdá, J. J.; Qiao, B.; Holm, C. *Eur. Phys. J. Spec. Top.* **2009**, *177*, 129–148.
(12) Reddy, G.; Yethiraj, A. *J. Chem. Phys.* **2010**, *132*, 074903.
(13) Farhat, T.; Yassin, G.; Dubas, S. T.; Schlenoff, J. B. *Langmuir* **1999**, *15*, 6621–6623.
(14) Rodriguez, L. N. J.; Paul, S. M. D.; Barrett, C. J.; Reven, L.; Spiess, H. W. *Adv. Mater.* **2000**, *12*, 1934–1938.
(15) Smith, R. N.; Reven, L.; Barrett, C. J. *Macromolecules* **2003**, *36*, 1876–1881.
(16) Dubas, S. T.; Schlenoff, J. B. *Macromolecules* **1999**, *32*, 8153–8160.
(17) Kovacevic, D.; van der Burgh, S.; de Keizer, A.; Cohen Stuart, M. A. *J. Phys. Chem. B* **2003**, *107*, 7998–8002.
(18) Bharadwaj, S.; Montazeri, R.; Haynie, D. T. *Langmuir* **2006**, *22*, 6093–6101.
(19) Laugel, N.; Betscha, C.; Winterhalter, M.; Voegel, J.-C.; Schaaf, P.; Ball, V. *J. Phys. Chem. B* **2006**, *110*, 19443–19449.
(20) Castelnovo, M.; Sens, P.; Joanny, J.-F. *Eur. Phys. J. E* **2000**, *1*, 115–125.
(21) Zhi, Z.-l.; Haynie, D. T. *Macromolecules* **2004**, *37*, 8668–8675.
(22) Itoh, K.; Tokumi, S.; Kimura, T.; Nagase, A. *Langmuir* **2008**, *24*, 13426–13433.
(23) Zhao, W.; Zheng, B.; Haynie, D. T. *Langmuir* **2006**, *22*, 6668–6675.
(24) Zhang, L.; Zhao, W.; Rudra, J. S.; Haynie, D. T. *ACS Nano* **2007**, *1*, 476–486.
(25) Hoda, N.; Larson, R. G. *Macromolecules* **2009**, *42*, 8851–8863.
(26) Lee, M. S.; Jr., F. R. S.; Olson, M. A. *J. Comput. Chem.* **2004**, *25*, 1967–1978.
(27) Peter, C.; Kremer, K. *Faraday Discuss.* **2010**, *144*, 9–24.
(28) Schlenoff, J. B.; Rmaile, A. H.; Bucur, C. B. *J. Am. Chem. Soc.* **2008**, *130*, 13589–13597.
(29) Spruijt, E.; Westphal, A. H.; Borst, J. W.; Cohen Stuart, M. A.; van der Gucht, J. *Macromolecules* **2010**, DOI: 10.1021/ma101031t.
(30) Chialvo, A. A.; Simonson, J. M. *J. Phys. Chem. C* **2008**, *112*, 19521–19529.
(31) Marcelo, G.; Tarazona, M. P.; Sai, E. *Polymer* **2004**, *45*, 1321–1330.
(32) Aldrich Catalog No. 40903−0.
(33) Hess, B.; Kutzner, C.; van der Spoel, D.; Lindahl, E. *J. Chem. Theory Comput.* **2008**, *4*, 435–447.
(34) Hess, B.; Bekker, H.; Berendsen, H. J. C.; Fraaije, J. G. E. M. *J. Comput. Chem.* **1997**, *18*, 1463–1472.
(35) Hess, B.; van der Vegt, N. F. A. *J. Phys. Chem. B* **2006**, *110*, 17616–17626.
(36) Berendsen, H. J. C.; Grigera, J. R.; Straatsma, T. P. *J. Phys. Chem.* **1987**, *91*, 6269–6271.
(37) Miyamoto, S.; Kollman, P. A. *J. Comput. Chem.* **1992**, *13*, 952–962.
(38) Jorgensen, W.; Maxwell, D.; Tirado-Rives, J. *J. Am. Chem. Soc.* **1996**, *118*, 11225–11236.
(39) Vishnyakov, A.; Neimark, A. V. *J. Chem. Phys.* **2008**, *128*, 164902–11.
(40) Thomas, A. S.; Elcock, A. H. *J. Am. Chem. Soc.* **2007**, *129*, 14887–14898.
(41) Martínez, J. M.; Martínez, L. *J. Comput. Chem.* **2003**, *24*, 819–825.
(42) Martínez, L.; Andrade, R.; Birgin, E. G.; Martínez, J. M. *J. Comput. Chem.* **2009**, *30*, 2157–2164.
(43) Darden, T.; York, D.; Pedersen, L. *J. Chem. Phys.* **1993**, *98*, 10089–10092.
(44) Essmann, U.; Perera, L.; Berkowitz, M. L.; Darden, T.; Lee, H.; Pedersen, L. *J. Chem. Phys.* **1995**, *103*, 8577.
(45) Bucur, C. B.; Sui, Z.; Schlenoff, J. B. *J. Am. Chem. Soc.* **2006**, *128*, 13690–13691.
(46) Jaber, J. A.; Schlenoff, J. B. *Langmuir* **2007**, *23*, 896–901.
(47) Crouzier, T.; Picart, C. *Biomacromolecules* **2009**, *10*, 433–442.
(48) Liu, X.; Bruening, M. L. *Chem. Mater.* **2004**, *16*, 351–357.
(49) Jin, W.; Toutianoush, A.; Tieke, B. *Appl. Surf. Sci.* **2005**, *246*, 444–450.
(50) Chávez, F. V.; Schönhoff, M. *J. Chem. Phys.* **2007**, *126*, 104705.
(51) Bockris, J. O.; Saluja, P. P. S. *J. Phys. Chem.* **1972**, *76*, 2140–2151.

(52) Brodholt, J. P. *Chem. Geol.* **1998**, *151*, 11–19.
(53) Kulcsar, A.; Voegel, J.-C.; Schaaf, P.; Kekicheff, P. *Langmuir* **2005**, *21*, 1166–1170.
(54) Hess, B.; Holm, C.; van der Vegt, N. *Phys. Rev. Lett.* **2006**, *96*, 147801.
(55) Hess, B.; Holm, C.; van der Vegt, N. *J. Chem. Phys.* **2006**, *124*, 164509.
(56) Gavryushov, S.; Linse, P. *J. Phys. Chem. B* **2006**, *110*, 10878–10887.
(57) de Leeuw, S. W.; Perram, J. W.; Smith, E. R. *Proc. R. Soc. London, A* **1980**, *373*, 27–56.
(58) Mahoney, M. W.; Jorgensen, W. L. *J. Chem. Phys.* **2000**, *112*, 8910–8922.
(59) Kusalik, P. G.; Mandy, M. E.; Svishchev, I. M. *J. Chem. Phys.* **1994**, *100*, 7654–7664.
(60) Neff, P. A.; Wunderlich, B. K.; von Klitzing, R.; Bausch, A. R. *Langmuir* **2007**, *23*, 4048–4052.
(61) Qiao, B.; Krekeler, C.; Berger, R.; DelleSite, L.; Holm, C. *J. Phys. Chem. B* **2008**, *112*, 1743–1751.
(62) Wende, C.; Schönhoff, M. *Langmuir* **2010**, *26*, 8352–8357.